

DEPARTMENT OF NATIONAL DEVELOPMENT
BUREAU OF MINERAL RESOURCES, GEOLOGY AND GEOPHYSICS

BULLETIN No. 119



**Standard Curves
for the
Magnetic Anomalies
due to Spheres**

BY
J. E. HAIGH



AUSTRALIAN GOVERNMENT PUBLISHING SERVICE
CANBERRA 1972

BUREAU OF MINERAL RESOURCES, GEOLOGY AND GEOPHYSICS

DIRECTOR: N. H. FISHER

ASSISTANT DIRECTOR, GEOPHYSICAL BRANCH: L. S. PRIOR

Published for the Minister for National Development,
the Hon. R. W. C. Swartz, M.B.E., E.D., M.P.,
by the Australian Government Publishing Service

ISBN 0 642 00109 X

CONTENTS

	Page
SUMMARY	1
1. INTRODUCTION	3
2. MATHEMATICAL DERIVATION	5
3. DISCUSSION	8
4. INTERPRETATION PROCEDURE	10
5. REFERENCES	10
TABLE 1. Values of the true amplitude, profiles of ΔZ and ΔX	11
TABLE 2. Values of true amplitude, profiles of ΔH	11
APPENDIX 1. Programme listings and flow charts	28

ILLUSTRATIONS

Figure 1. Definition of axes	4
Figure 2. Distribution of field components	4
Plate 1. Nomogram for determination of effective inclination	12
Plate 2. Magnetic anomalies over a sphere—Vertical component (Z)	13
Plate 3. Magnetic anomalies over a sphere—Horizontal component in the traverse direction (X)	14
Plates 4-13. Magnetic anomalies over a sphere—Horizontal component (H)	15-24
Plate 14. Nomogram for determination of the parameter C	25
Plate 15. Nomogram for determination of the radius of the sphere	26
Plate 16. Examples of the application of the curves for ΔZ	27

SUMMARY

Standard curves for interpretation of the magnetic anomalies due to spheres have been derived. The anomalies in the vertical component, and the horizontal component in the direction of the traverse, are each found to be represented by a single family of curves. The horizontal component is found to be not represented by a single family, and separate curves for each field inclination and traverse azimuth are presented. Curves for the anomaly in the total intensity were not computed.

Page 2 is blank.

1. INTRODUCTION

The relative merits of the various methods of magnetic interpretation have been discussed by Gay (1963, 1965). The advantages of the curve fitting methods are obvious, since a high proportion of the data is used. The use of the curve fitting method presupposes the availability of a sufficiently varied set of standard curves. Gay (1963, 1965) has published curves for infinite dykes and horizontal cylinders. However, it is generally accepted that many of the magnetic bodies found in nature are approximately spherical. Gay (1965) pointed out the need for a complete set of standard curves of magnetic anomalies due to spheres but observed that 'anomalies over spheres have not proven to be representable by a single family of curves, a characteristic reserved only for two-dimensional bodies'.

The Bureau of Mineral Resources, Geology & Geophysics has conducted extensive ground magnetic surveys using only the vertical component, and interest in improving the interpretation of such surveys led to the search for a family of curves to represent the vertical-component anomaly due to a sphere. It has been found that the vertical-intensity anomaly ΔZ for all field inclinations and traverse directions can be represented by a single family of curves. The horizontal-intensity anomaly in the direction of the traverse (ΔX) can similarly be represented by a single family of curves. The horizontal-intensity anomaly in the north direction (ΔH) cannot be represented by a single family but requires a separate curve for each value of field inclination and traverse direction. The standard curves derived for ΔZ , ΔX , and ΔH are presented in Plates 2 to 15.

No attempt was made to derive the total-field anomaly due to a sphere.

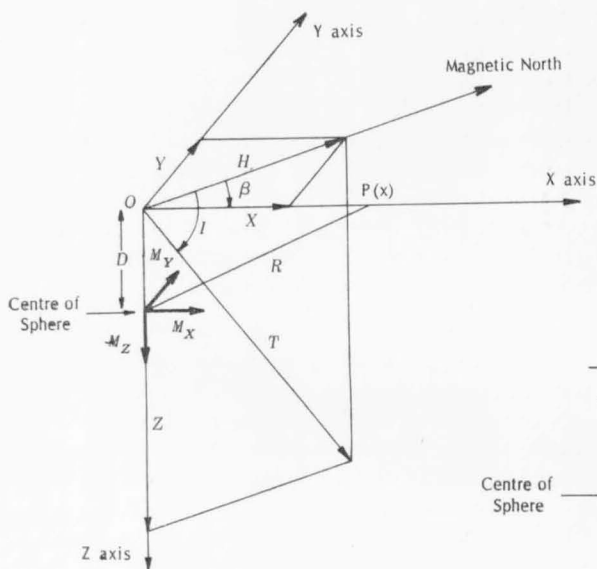


Figure 1. Definition of axes

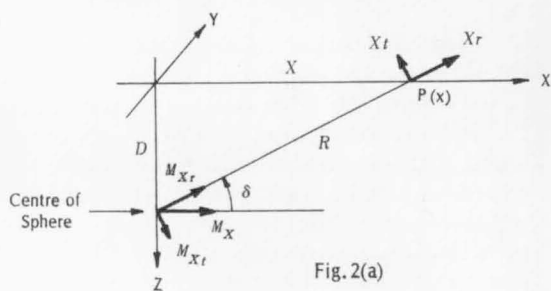
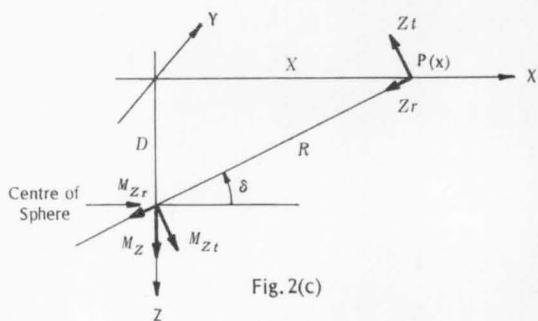
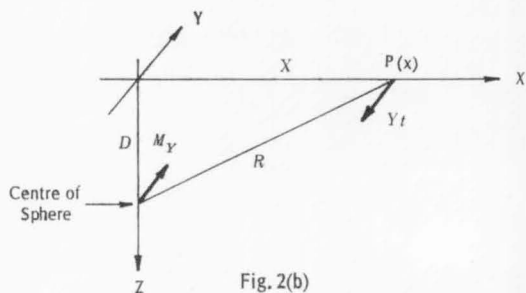


Figure 2. Distribution of field components



2. MATHEMATICAL DERIVATION

Consider a left-handed orthogonal co-ordinate system (Fig. 1) with its origin on the surface of the Earth directly above the centre of a small, uniformly magnetised sphere at unit depth, such that X is positive in the traverse direction at an azimuth angle β clockwise from magnetic north and Z is positive vertically downwards. The magnetic moment M induced in the sphere by the magnetic field T of inclination I may be resolved into components M_x, M_y, M_z along the X, Y , and Z axes respectively. At any point P on the traverse, distant x from the origin, these components may each be further resolved into radial and tangential components, which at P give rise to the magnetic field components defined in Figure 2. Defining Z_x as the field component at P in the Z direction due to the moment M_x , and similarly for other components, the net effect at P may be written directly from the basic theory of the magnetic dipole (Jakosky, 1961, p. 79):

$$\begin{aligned} Z_x &= \frac{-2 M_{xr}}{R^3} \sin \delta - \frac{M_{xt}}{R^3} \cos \delta \\ &= \frac{-2 M_x \cos \delta \sin \delta - M_x \sin \delta \cos \delta}{R^3} \\ &= \frac{-3 M \cos I \cos \beta \cos \delta \sin \delta}{R^3} \\ &= \frac{-3 M \cos I \cos \beta x d}{R^5} \end{aligned}$$

$$\begin{aligned} X_x &= \frac{2 M_{xr}}{R^3} \cos \delta - \frac{M_{xt}}{R^3} \sin \delta \\ &= \frac{2 M_x \cos \delta \cos \delta - M_x \sin \delta \sin \delta}{R^3} \\ &= \frac{2 M_x x^2 - M_x d^2}{R^5} \\ &= \frac{M \cos I \cos \beta (2x^2 - d^2)}{R^5} \end{aligned}$$

$$Y_x = 0$$

$$Z_y = 0$$

$$X_y = 0$$

$$Y_y = \frac{-M_y}{R^3} = \frac{-M \cos I \sin \beta}{R^3}$$

$$\begin{aligned} Z_z &= \frac{2 M_{zr}}{R^3} \sin \delta - \frac{M_{zt}}{R^3} \cos \delta \\ &= \frac{2 M_z \sin \delta \sin \delta - M_z \cos \delta \cos \delta}{R^3} \\ &= \frac{M \sin I (2 d^2 - x^2)}{R^5} \end{aligned}$$

$$\begin{aligned}
X_z &= \frac{-2 M_{zr}}{R^3} \cos \delta - \frac{M_{zt}}{R^3} \sin \delta \\
&= \frac{-2 M_z \sin \delta \cos \delta - M_z \cos \delta \sin \delta}{R^3} \\
&= \frac{-3 M \sin I \sin \delta \cos \delta}{R^3} \\
&= \frac{-3 M \sin I x d}{R^5}
\end{aligned}$$

$$Y_z = 0$$

The net components of magnetic intensity in the X, Y, and Z directions are:

$$\begin{aligned}
\Delta X &= \frac{-3 M \sin I x d + M \cos I \cos \beta (2x^2 - d^2)}{R^5} \\
\Delta Y &= \frac{-M \cos I \sin \beta}{R^3} \\
\Delta Z &= \frac{M \sin I (2d^2 - x^2) - 3 M \cos I \cos \beta x d}{R^5}
\end{aligned}$$

and the net horizontal component is:

$$\Delta H = \Delta X \cos \beta + \Delta Y \sin \beta$$

Gay (1963) after Koulomzine and Massé (1947) has defined the effective magnetic inclination in the direction of the traverse (E), and the same approach is followed in this derivation. A nomogram for the determination of effective inclination is shown in Plate 1. The traverse azimuth β may be eliminated from the above equations by use of the relation:

$$\cos \beta = \frac{\tan I}{\tan E}$$

and, defining d to be unit distance and S and Q such that:

$$\begin{aligned}
x &= S d \\
R &= Q d
\end{aligned}$$

we have:

$$\begin{aligned}
\Delta Z &= \frac{M}{d^3} \cdot \frac{\sin I}{\sin E} \cdot \frac{(2 - S^2) \sin E - 3 S \cos E}{Q^5} \\
&= \frac{K (2 - S^2) \sin E - 3 S \cos E}{Q^5} \\
&= K (f(S)) \\
\Delta X &= \frac{M}{d^3} \cdot \frac{\sin I}{\sin E} \cdot \frac{(2 S^2 - 1) \cos E - 3 S \sin E}{Q^5} \\
&= K (g(S))
\end{aligned}$$

The functions for ΔZ , ΔX , and ΔH were computed and machine plotted using a 'CDC 3600' computer and 'Calcomp' graph plotter. Programme listings and flow charts are given in Appendix 1.

The plotted curves were normalised to have unit amplitude. The true amplitude a for each curve is listed in Table 1 or Table 2. The magnitude A of the field anomaly in gammas is related to K and a by:

$$A = K a$$

$$\text{Now } M = \frac{4}{3} \pi r^3 k T$$

$$A = \frac{4 \pi r^3 k T a \sin I}{3 d^3 \sin E}$$

where r is the radius of the sphere, k is the susceptibility contrast, and T is the total intensity of the Earth's field.

$$\therefore r^3 k = \frac{(3 A \sin E) d^3}{4 \pi a T \sin I} = C d^3$$

The value of $(\sin E)/(T \sin I)$ will normally be constant within a given survey area. The value of the parameter C may be calculated or may be obtained from the nomogram in Plate 14. If the value of k is known or estimated, a value for the radius of the sphere may then be obtained from the nomogram in Plate 15.

For profiles of the horizontal-intensity anomaly the value of C is as above except that the $(\sin E)/(\sin I)$ term is always 1.0.

The profiles as presented are for the northern hemisphere (north to the right) and may be converted to southern hemisphere profiles by transposing them from left to right. The profiles for Z may also be inverted depending on the plotting convention adopted for the observed profiles. In the southern hemisphere it is customary to plot $-Z$ upwards in order to produce anomalies that 'look' right; in this case the theoretical profiles should not be inverted.

3. DISCUSSION

A discrete point method of interpreting magnetic anomalies due to spheres has been described by Daly (1957), who also described methods of calculating the theoretical curve for any given interpretation. However, this is quite tedious and would not normally be carried out in routine interpretation. The present method gives a rapid interpretation for the anomalies due to spheres, and also gives a measure of the reliability of the method from the degree of fit between the observed values and the theoretical curve.

The method of interpretation by curve superposition has been adequately described by Gay (1963, 1965), and the curves as presented here need little discussion.

As shown in the derivation, anomalies in ΔZ and ΔX are represented by separate families of curves (Plates 2 and 3), but the anomaly in ΔH requires a separate curve for each field inclination and traverse azimuth (Plates 4 to 13). It is obvious from the plates that in high magnetic latitudes, measurements of ΔH should not be taken on traverses that lie near an east-west direction; on such traverses, variations of only one or two degrees in azimuth cause large variations in the anomaly profile.

In planning a survey where horizontal magnetic measurements are to be made direct, consideration should be given to the desirability of measuring ΔX rather than ΔH . Measurements of ΔX can be made with a Schmidt balance, torsion magnetometer, or horizontal fluxgate magnetometer; all these instruments measure the horizontal intensity in the azimuth to which they are constrained. Interpretation of the anomalies in ΔX can be simply carried out using the single family of curves shown in Plate 3. There is still a restriction on the allowable traverse azimuth, imposed by the errors that may be introduced by mis-orientation of the instrument. For example, in a horizontal field of 25,000 gammas, with a traverse azimuth of 30° , a mis-orientation of one tenth of a degree introduces an error of about 20 gammas in ΔX ; if the traverse azimuth is 60° , the error increases to about 37 gammas. Nevertheless, if a suitable sighting device were attached to the instrument, accurate orientation should not prove difficult.

Chapter 4 gives a summarised step-by-step procedure for using the standard curves in the interpretation of magnetic anomalies.

Two examples of the application of the curves for ΔZ are shown in Plate 16. Both are extracted from examples from the Tennant Creek area given by Daly (1957). In both cases the degree of fit of the observed points is only moderate, indicating that the sources of the anomalies are not actually spherical.

Example 1 is from Traverse 500W of the Eldorado anomaly. Daly's estimated depth to the centre of the body was 580 feet, which agrees well with the present determination (570 feet). However, Daly places the centre of the body below point 402N, whereas the present determination places it below 430N. The amplitude A of the anomaly is 1600 gammas. Referring to Table 1, the true amplitude a of the theoretical curve is 1.92. Taking $F = 50,000$ gammas, $(\sin E)/(T \sin I) = 2 \times 10^{-5}$. From the nomogram in Plate 14, $C = 4.0 \times 10^{-3}$. Daly has dis-

cussed the likely values for the susceptibility contrast of the ironstones at Tennant Creek, and he suggests that the most probable value is $k = 0.1$ c.g.s. units. Thus for a depth of 570 feet, the radius of the sphere is 200 feet (Plate 15).

In Example 2, Daly's estimated position for the centre of the sphere was at a depth of 410 feet below point 400S. The present determination places it at a depth of 500 feet below 410S. The amplitude of the anomaly is 3900 gammas, which gives values of $C = 9.5 \times 10^{-3}$ and $r = 250$ feet.

It is interesting to note that the interpretations using the two methods give different results even though they are based on the same basic theory. This is attributed to the difference between the discrete point method and the complete curve fitting method.

4. INTERPRETATION PROCEDURE

To permit rapid interpretation of profiles using this method, it is recommended that the step-by-step procedure set out below be followed.

- (1) Plot field results at a convenient scale.
- (2) For profiles of ΔZ or ΔX , determine the value of effective inclination E from the field inclination I and traverse azimuth β , using the nomogram in Plate 1, and select the theoretical curve appropriate to the value of E .
For profiles of ΔH , select the theoretical curve appropriate to the values of I and β .
- (3) Change the vertical scale of the observed profile so that the amplitude (peak-to-peak) is the same as that of the theoretical profile.
- (4) Vary the horizontal scale of the observed profile to obtain the best fit between it and the theoretical profile (it may be necessary to repeat steps 3 or 4 to obtain the best possible fit between the two sets of curves).
- (5) The depth to the centre of the sphere is that distance on the horizontal scale of the observed profile which corresponds to one unit on the horizontal scale of the theoretical profile.
- (6) Measure the gamma amplitude A of the observed profile, and from Table 1 or Table 2 obtain the true amplitude a of the theoretical profile.
- (7) Compute $(\sin E)/(T \sin I)$.
- (8) From the equation on page 7 or from the nomogram in Plate 14, obtain a value for C .
- (9) From the value of C obtained in step 8, and a selected value of susceptibility contrast k , determine the value of the radius r from the nomogram in Plate 15.

5. REFERENCES

- ALLCOCK, H. J., and JONES, J. R., 1946—THE NOMOGRAM. London, Pitman & Sons, 3rd edition.
- DALY, J., 1957—Magnetic prospecting at Tennant Creek, Northern Territory 1935-37. *Bur. Min. Resour. Aust. Bull.*, 44.
- GAY, S. P., 1963—Standard curves for interpretation of magnetic anomalies over long tabular bodies. *Geophysics*, 28 (2), pp. 161-200.
- GAY, S. P., 1965—Standard curves for magnetic anomalies over long horizontal cylinders. *Geophysics*, 30 (5), pp. 818-828.
- JAKOSKY, J. J., 1961—EXPLORATION GEOPHYSICS. Newport Beach, California, Trija Publishing Co., 3rd Edition.
- KOULOMZINE, Th., and MASSE, L., 1947—Magnetic anomaly of inclined vein of infinite length. *Amer. Inst. Min. Engrs. Technical Publication No. 2260*.

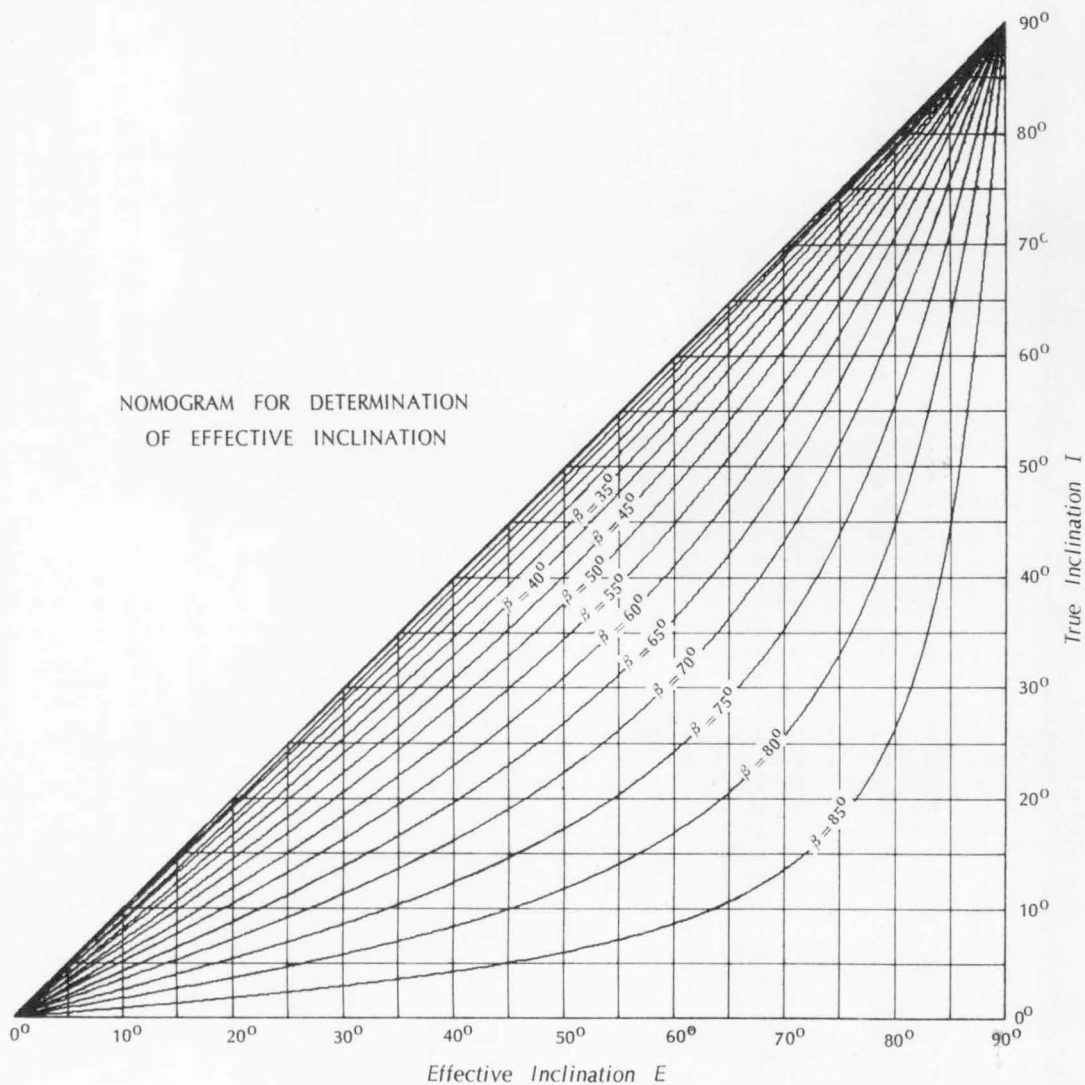
TABLE 1. VALUES OF TRUE AMPLITUDE a

Profiles of ΔZ		Profiles of ΔX	
Effective inclination	True amplitude	Effective inclination	True amplitude
0°	1.7173	0°	1.2024
10°	1.7275	10°	1.2712
20°	1.7579	20°	1.3467
30°	1.8043	30°	1.4255
40°	1.8609	40°	1.5022
50°	1.9210	50°	1.5725
60°	1.9759	60°	1.6326
70°	2.0176	70°	1.6784
80°	2.0398	80°	1.7074
90°	2.0358	90°	1.7173

TABLE 2. VALUES OF TRUE AMPLITUDE a . PROFILES OF ΔH .

Inclination	Traverse Azimuth	True Amplitude	Inclination	Traverse Azimuth	True Amplitude	Inclination	Traverse Azimuth	True Amplitude
0°	0°	1.2024	10°	0°	1.2712	20°	0°	1.3467
	10°	1.1887		10°	1.2550		10°	1.3282
	20°	1.1506		20°	1.2089		20°	1.2751
	30°	1.0962		30°	1.1412		30°	1.1944
	40°	1.0401		40°	1.0658		40°	1.0988
	50°	1.0038		50°	1.0060		50°	1.0091
	60°	1.0000		60°	.9922		60°	.9692
	70°	1.0000		70°	.9891		70°	.9568
	80°	1.0000		80°	.9861		80°	.9448
	90°	1.0000		90°	.9848		90°	.9397
30°	0°	1.4255	40°	0°	1.5022	50°	0°	1.5724
	10°	1.4050		10°	1.4799		10°	1.5488
	20°	1.3452		20°	1.4148		20°	1.4793
	30°	1.2526		30°	1.3118		30°	1.3679
	40°	1.1376		40°	1.1797		40°	1.2217
	50°	1.0171		50°	1.0315		50°	1.0505
	60°	.9310		60°	.8913		60°	.8703
	70°	.9039		70°	.8321		70°	.7437
	80°	.8778		80°	.7877		80°	.6775
	90°	.8660		90°	.7660		90°	.6428
60°	0°	1.6326	70°	0°	1.6784	80°	0°	1.7074
	10°	1.6079		10°	1.6529		10°	1.6815
	20°	1.5350		20°	1.5775		20°	1.6045
	30°	1.4170		30°	1.4550		30°	1.4789
	40°	1.2598		40°	1.2898		40°	1.3088
	50°	1.0706		50°	1.0878		50°	1.0995
	60°	.8611		60°	.8584		60°	.8582
	70°	.6533		70°	.6133		70°	.5934
	80°	.5520		80°	.4168		80°	.3195
	90°	.5000		90°	.3420		90°	.1736
			90°	0°	1.7173			
				10°	1.6912			
				20°	1.6137			
				30°	1.4872			
				40°	1.3155			
				50°	1.1039			
				60°	.8586			
				70°	.5873			
				80°	.2982			

NOMOGRAM FOR DETERMINATION
OF EFFECTIVE INCLINATION



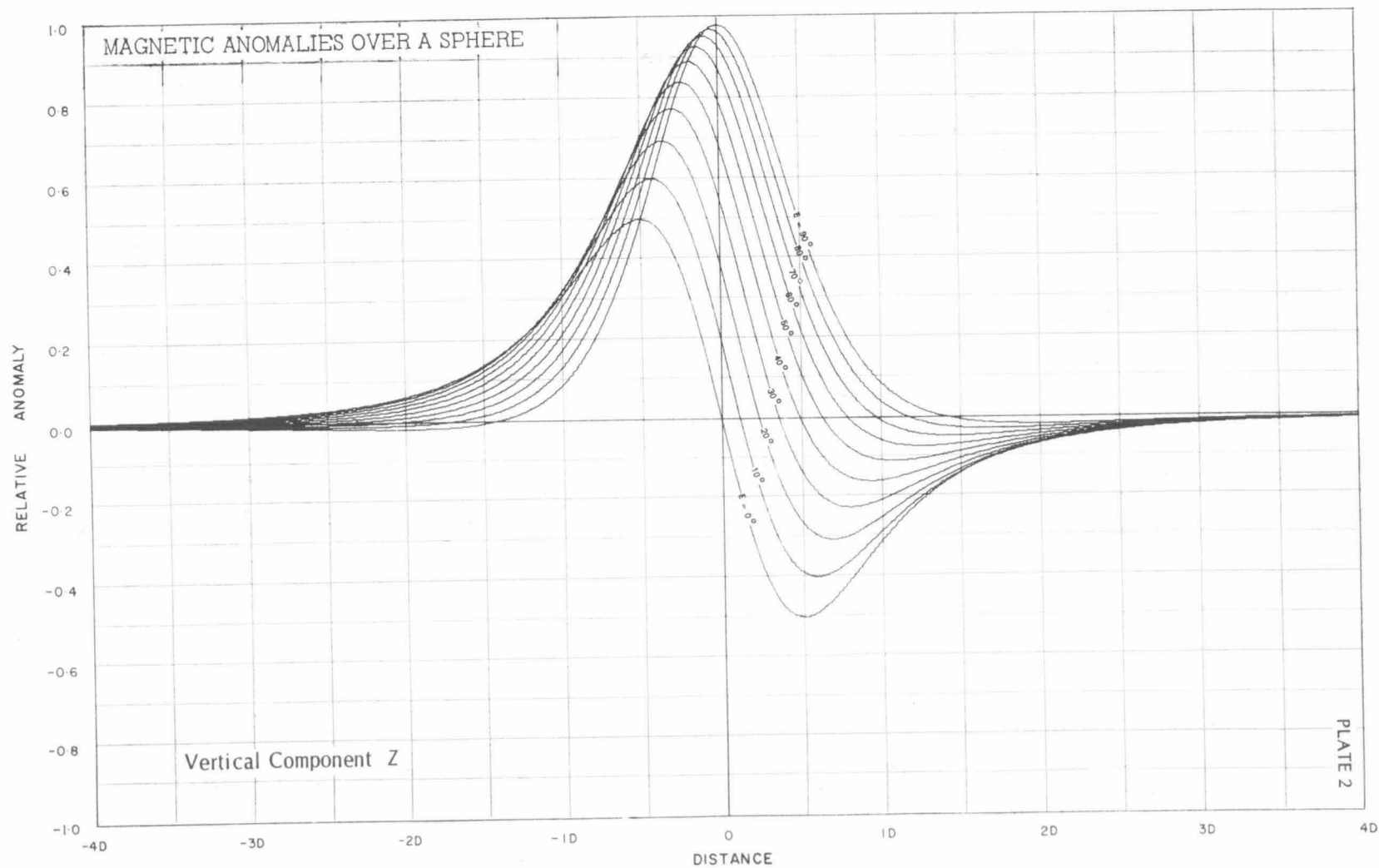
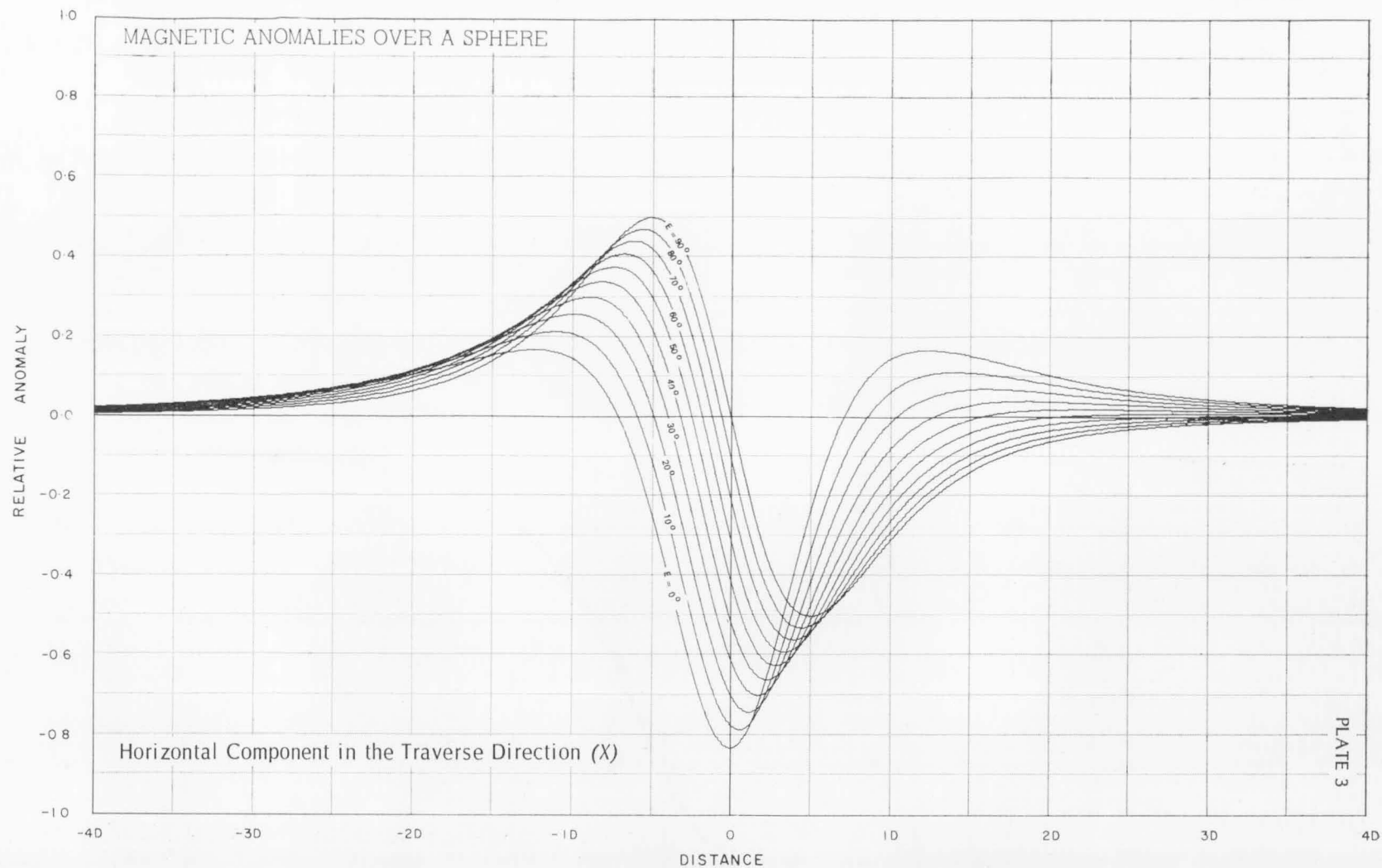
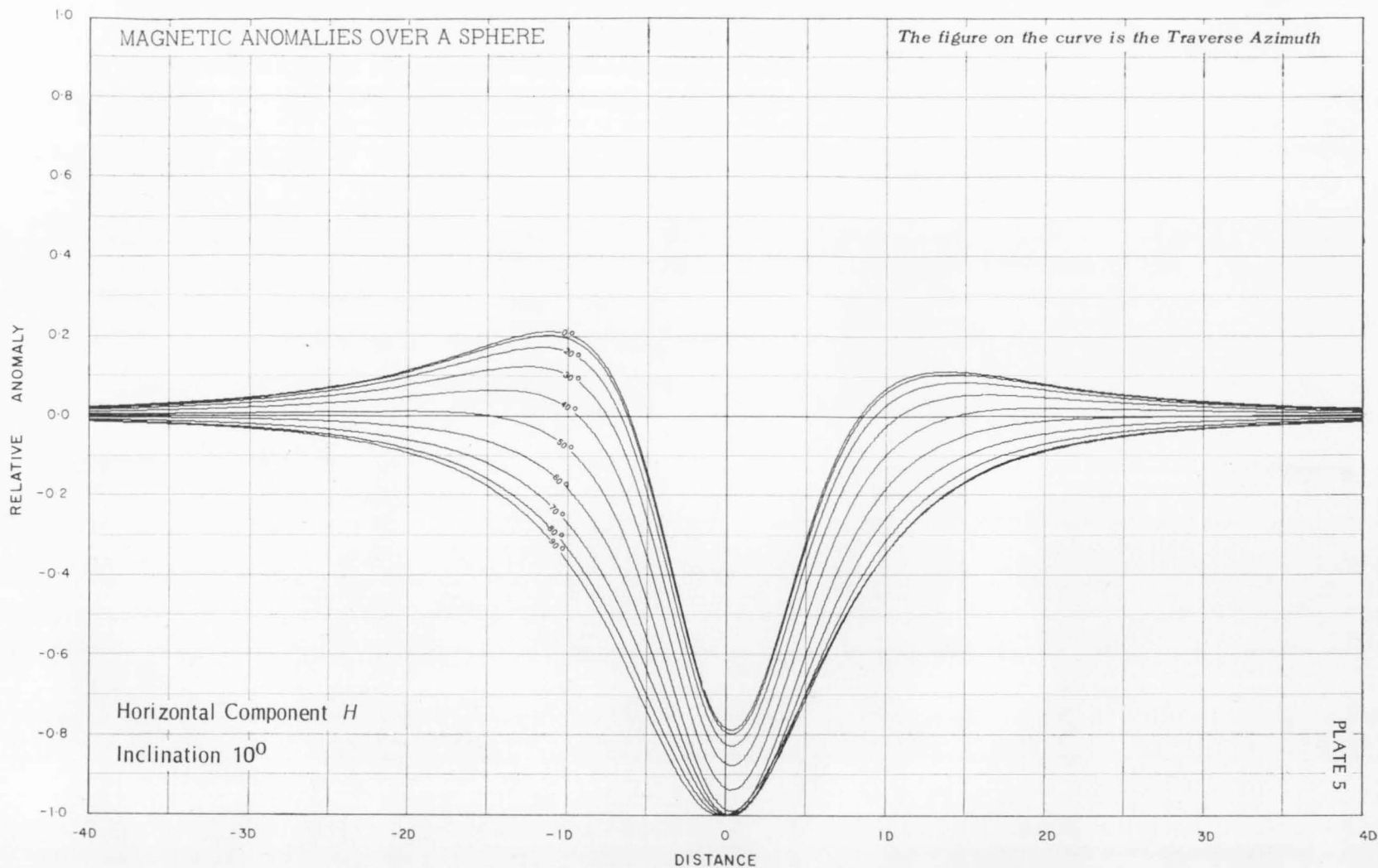
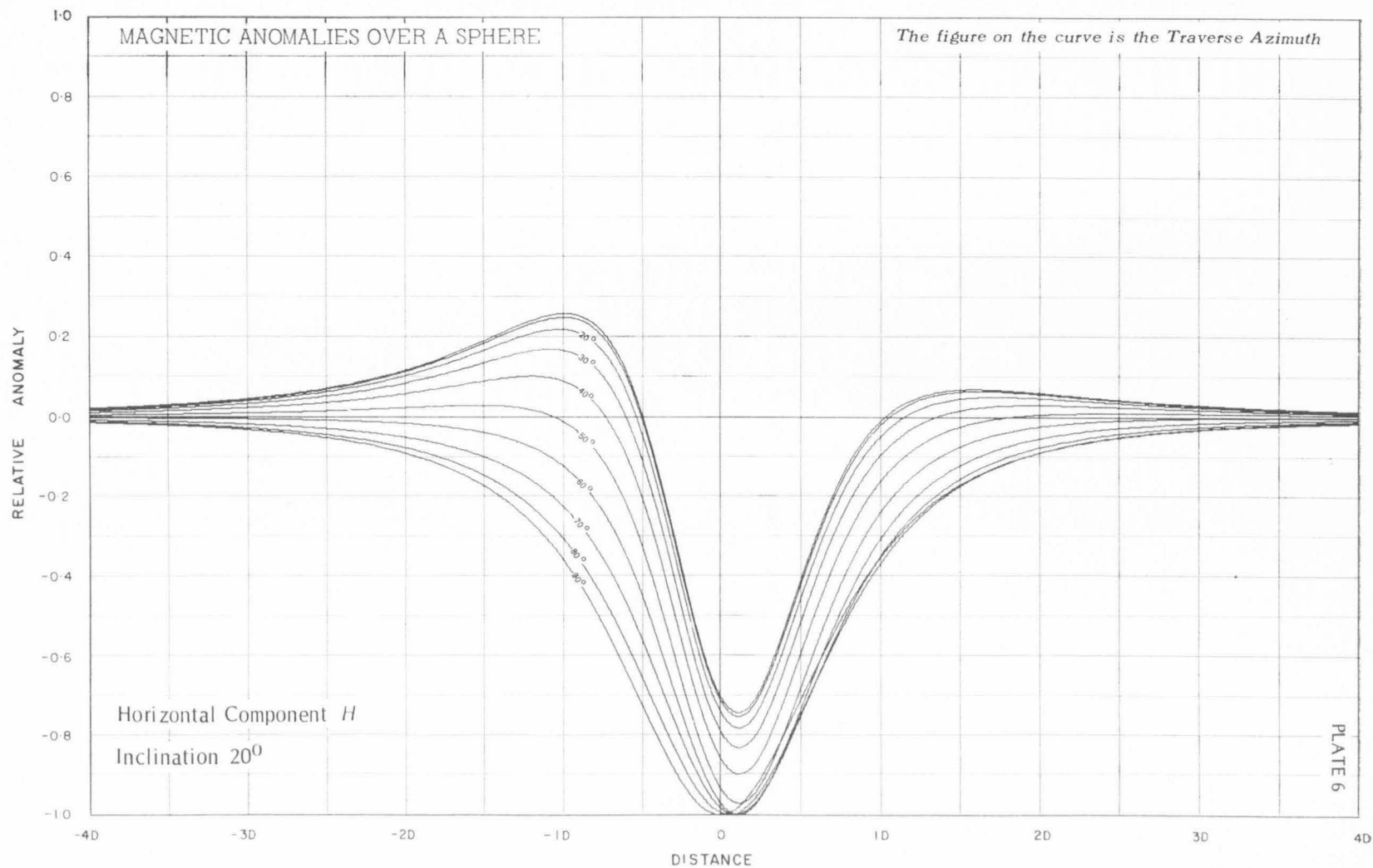
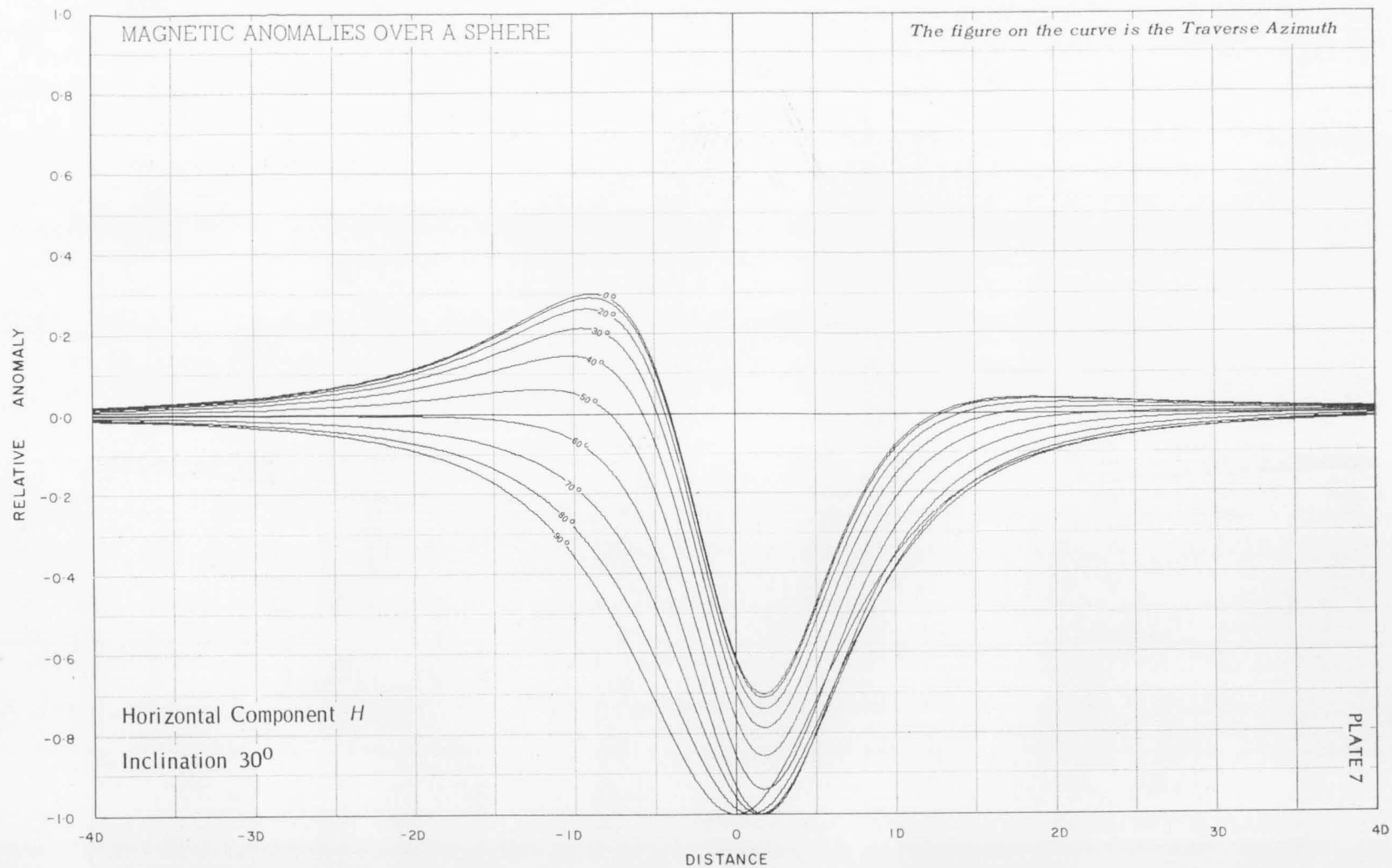


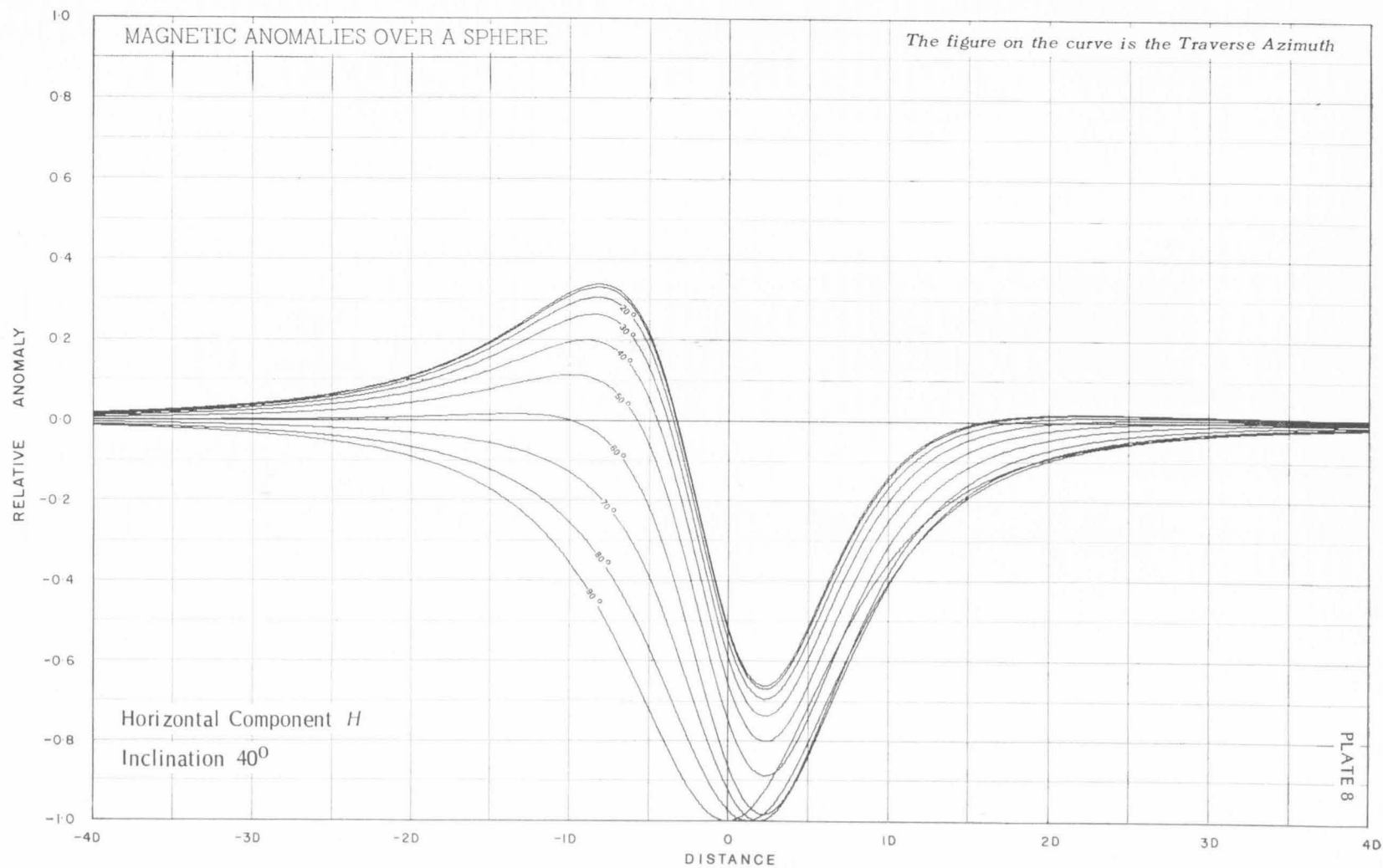
PLATE 2

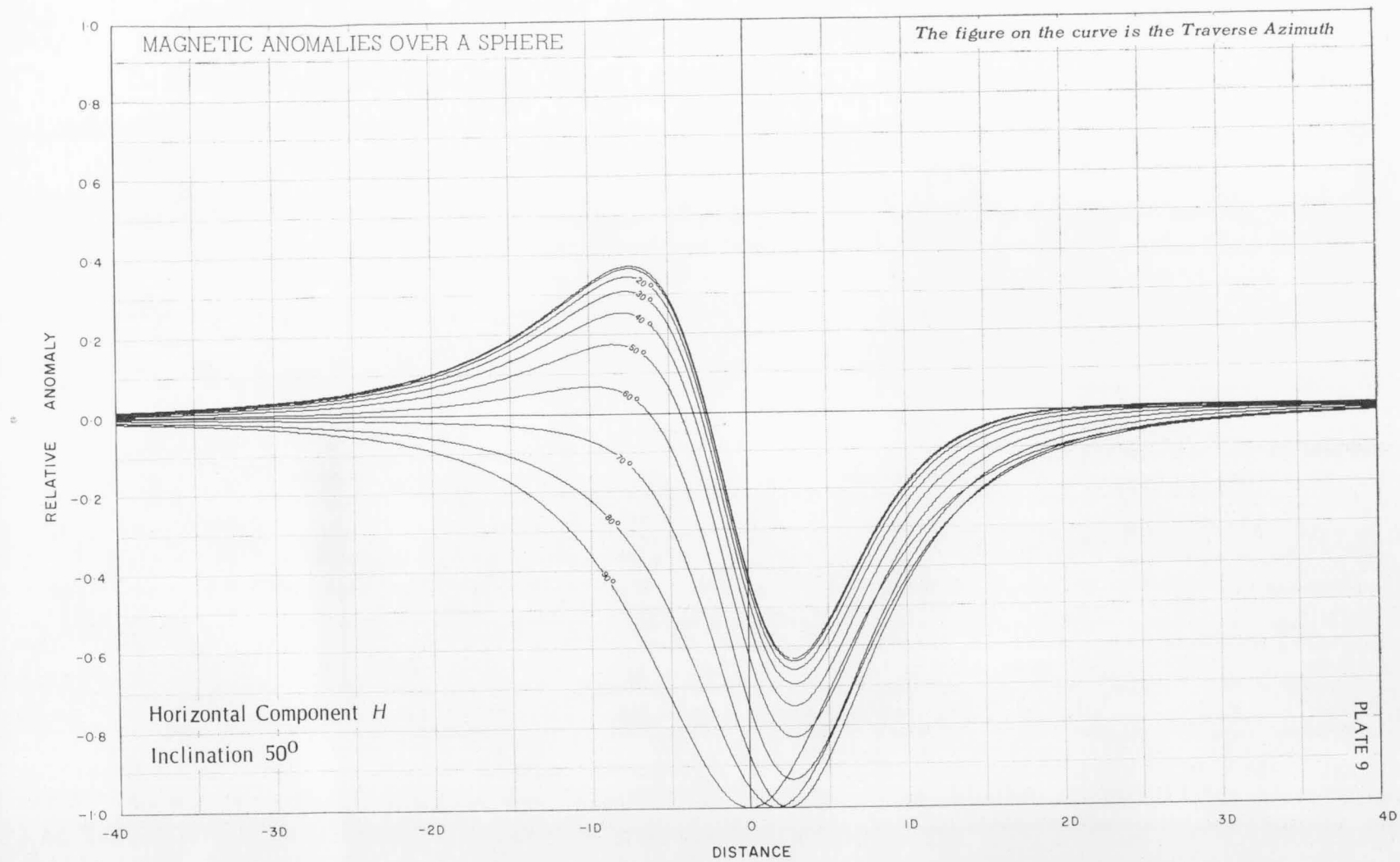


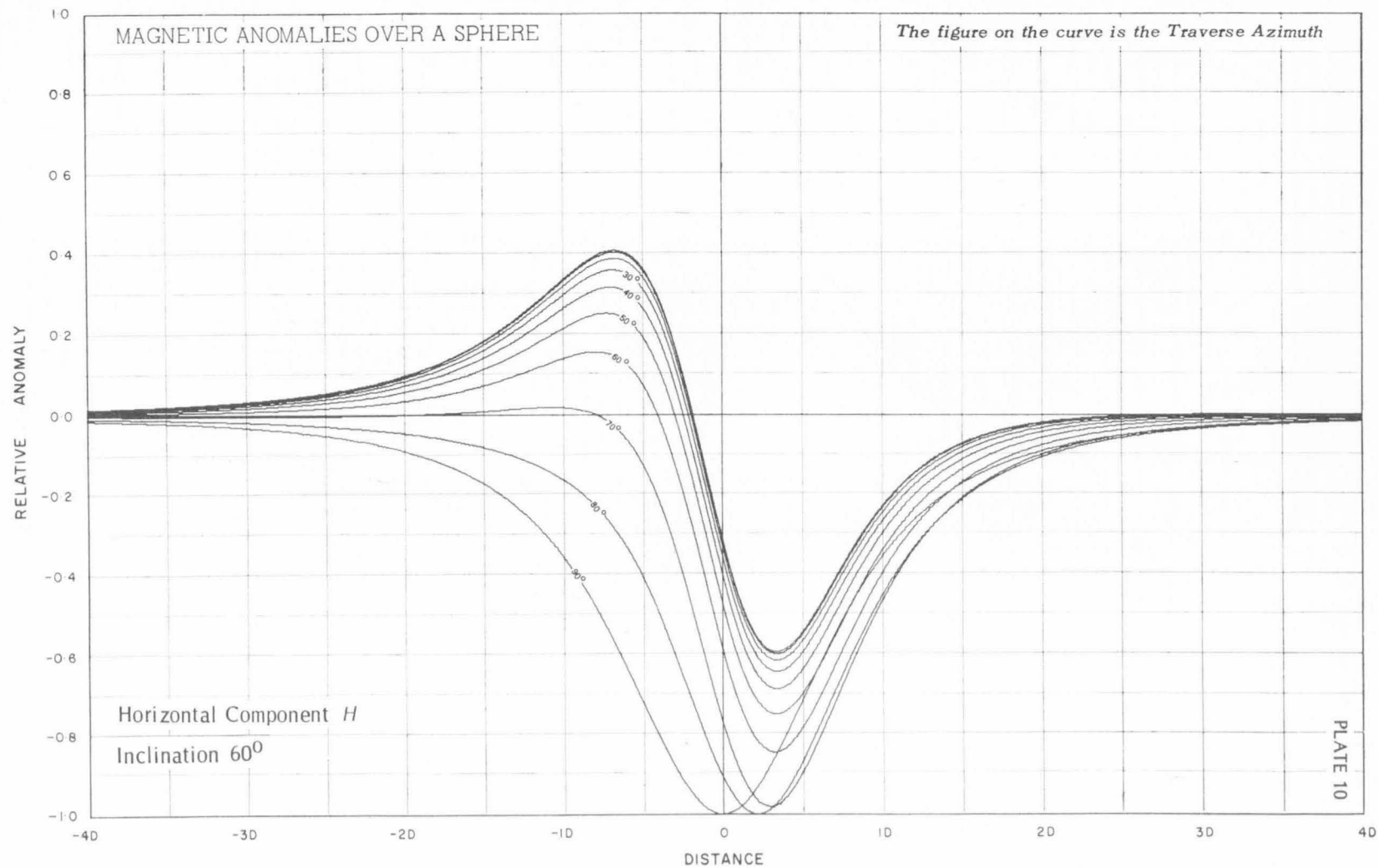


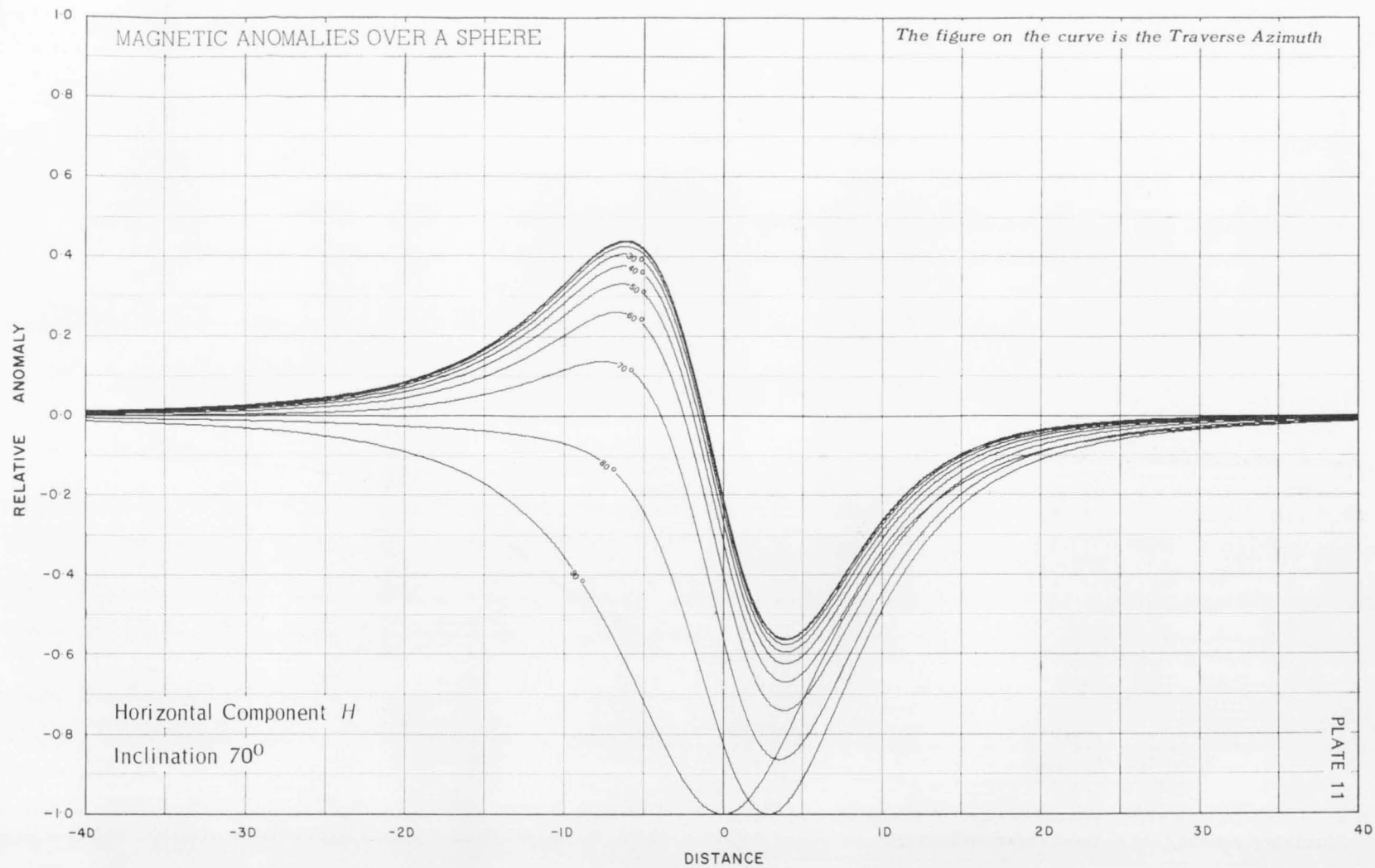






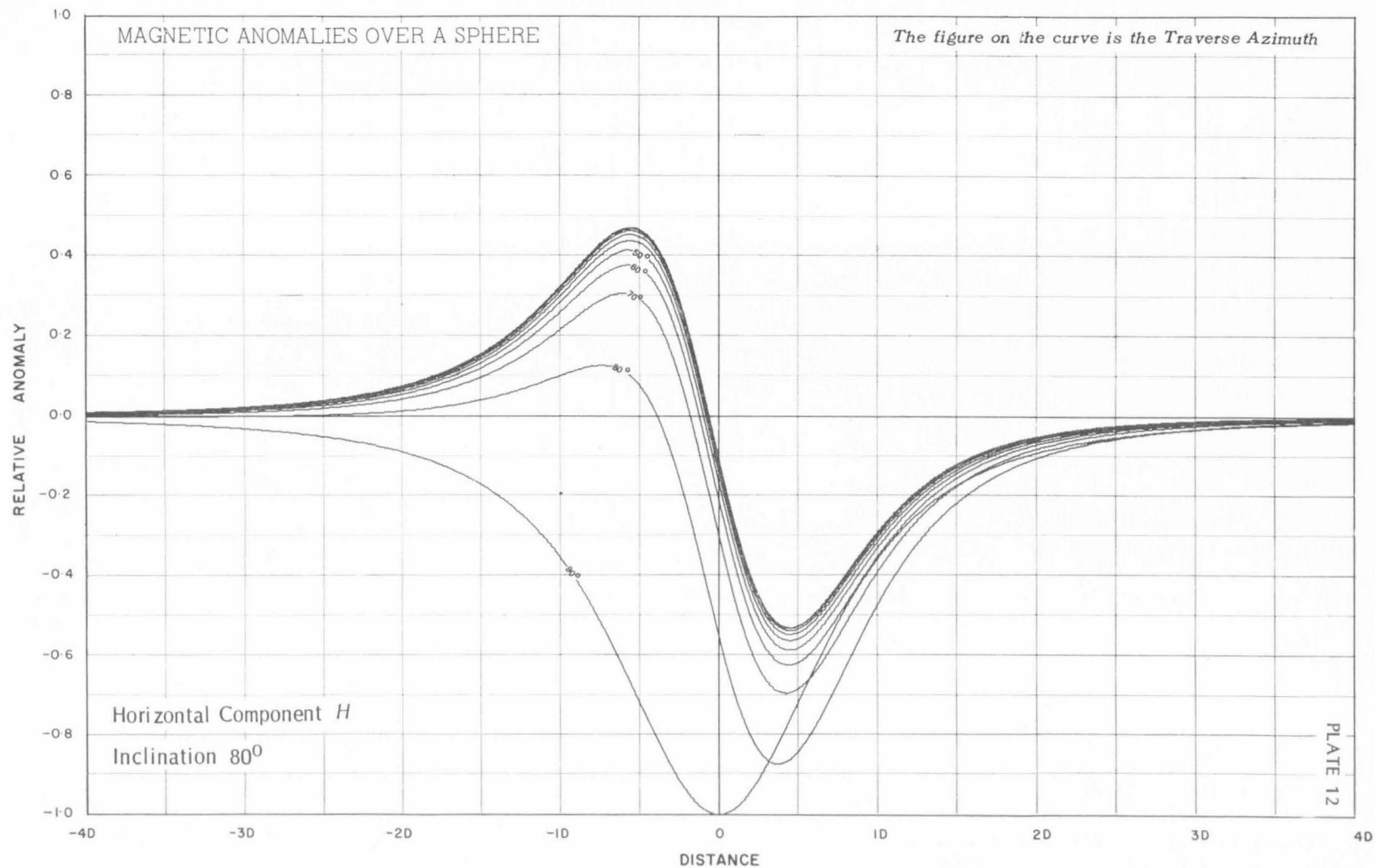


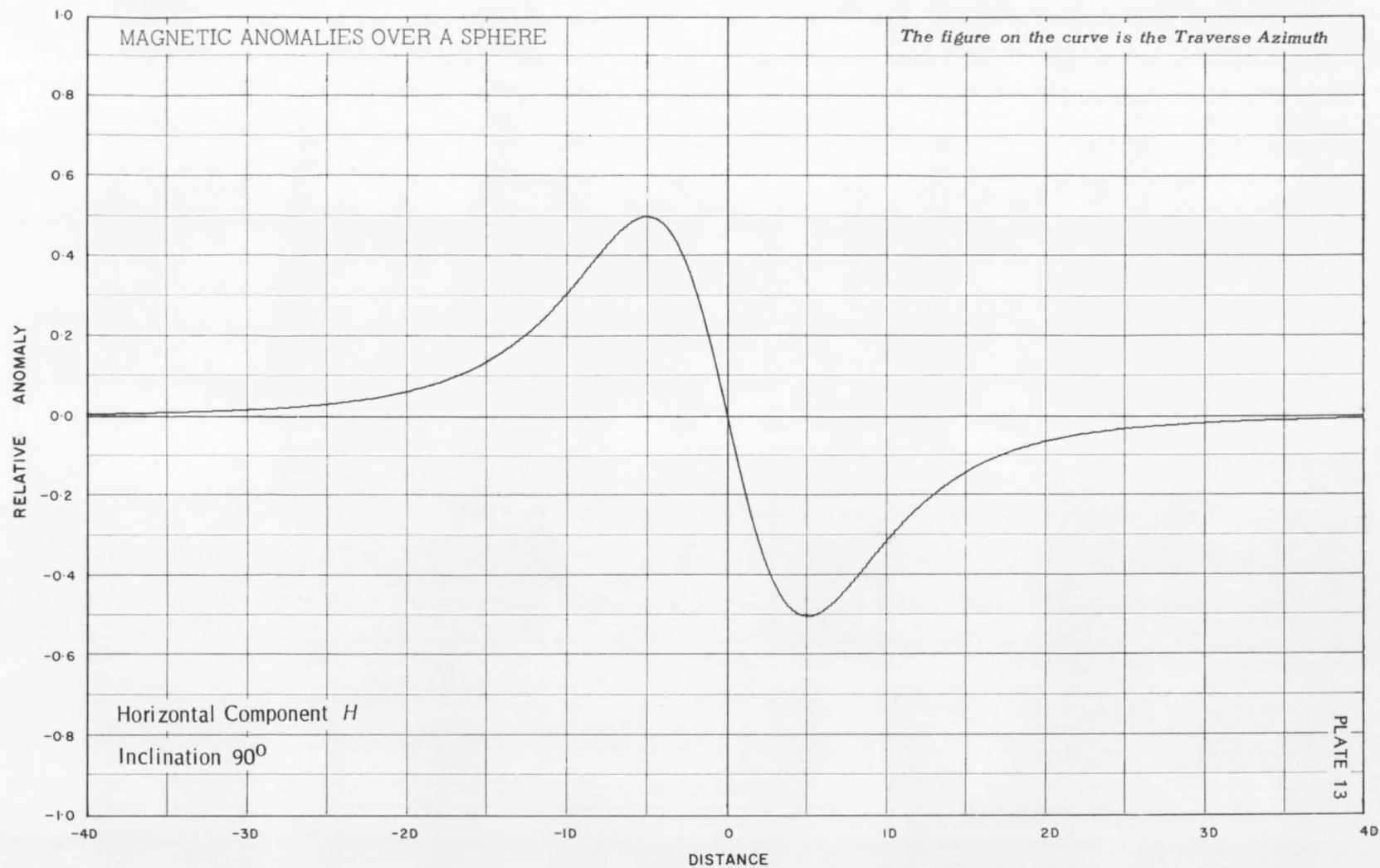


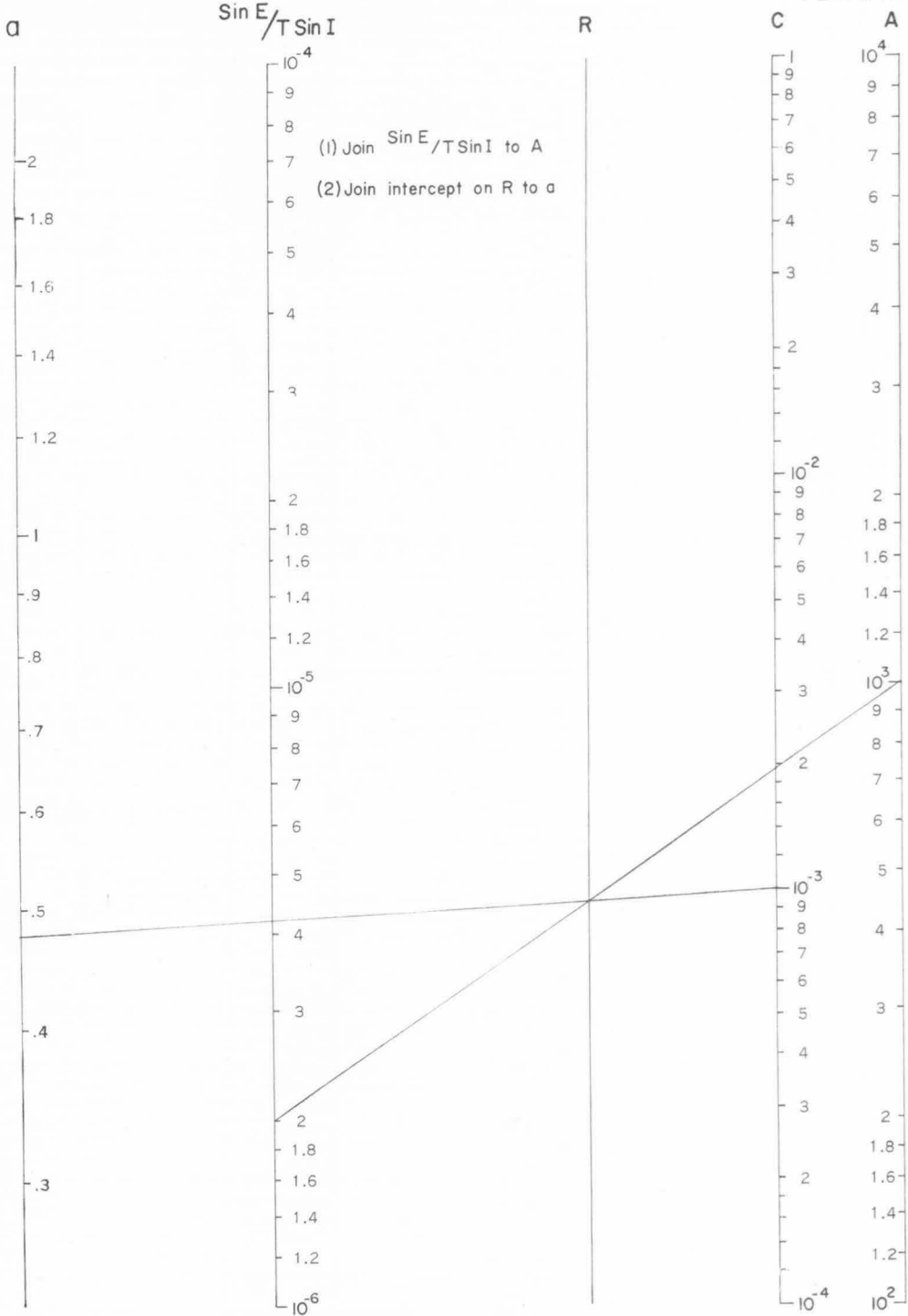


MAGNETIC ANOMALIES OVER A SPHERE

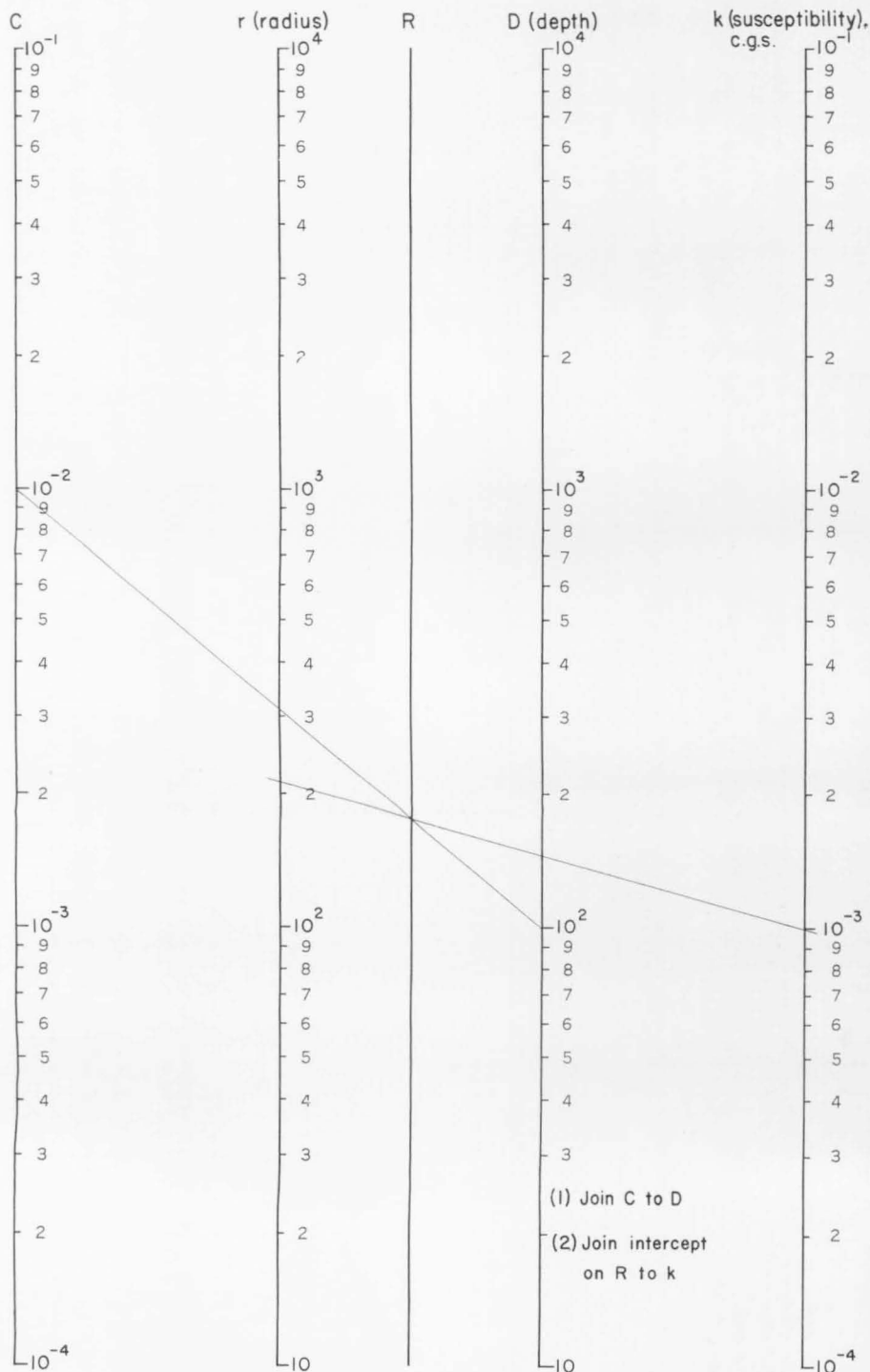
The figure on the curve is the Traverse Azimuth



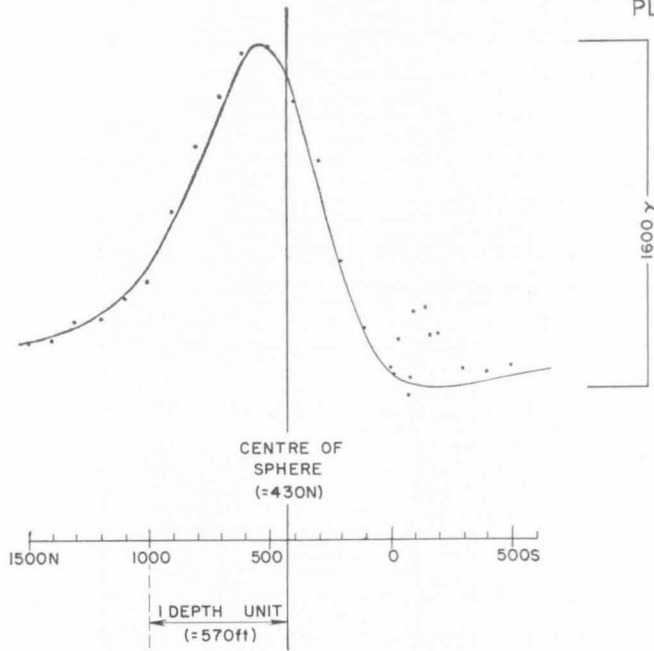




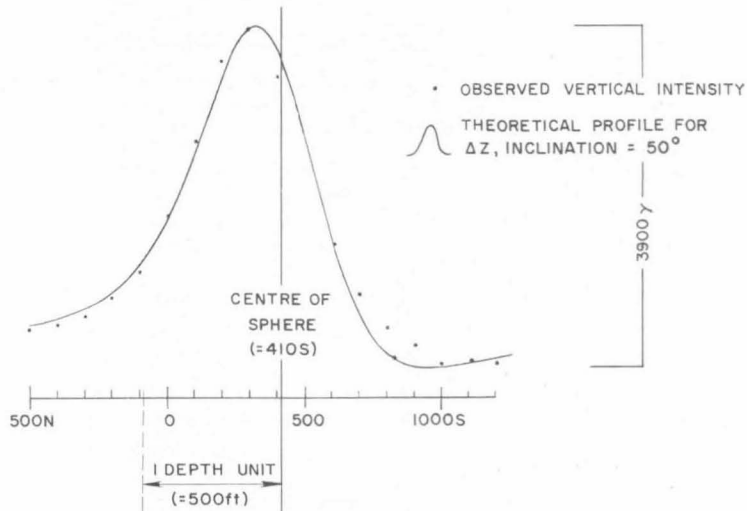
NOMOGRAM FOR DETERMINATION OF PARAMETER C



NOMOGRAM FOR DETERMINATION OF RADIUS OF A MAGNETISED SPHERE



(1) "ELDORADO" TRAV 500W TENNANT CK AREA
(AFTER DALY 1957)



(2) "PEKO" TRAV 3400E TENNANT CK AREA
(AFTER DALY 1957)

EXAMPLES OF THE APPLICATION OF THE CURVES FOR ΔZ

APPENDIX 1

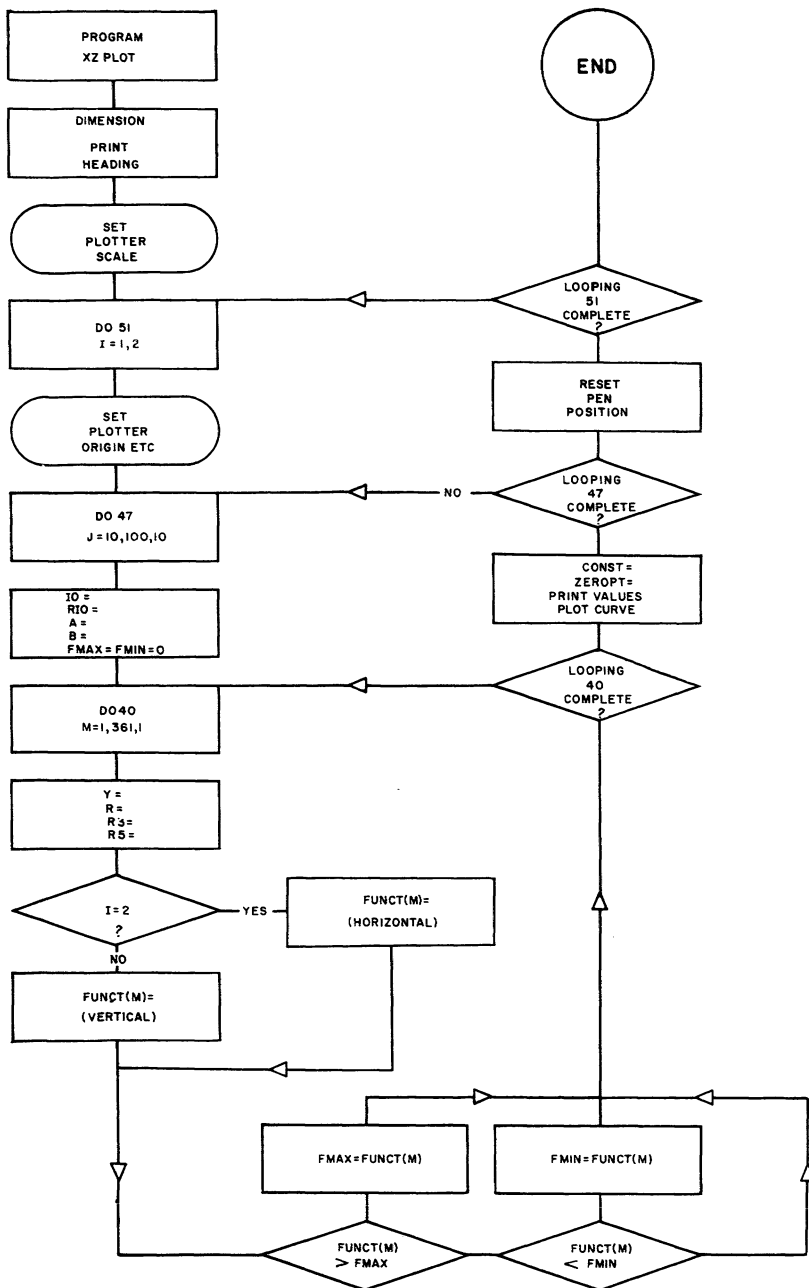
PROGRAMME LISTINGS AND FLOW CHARTS

Computer programme listings and flow charts used in the computations described in this Bulletin appear on the next four pages.

```

PROGRAM XZPLOT
DIMENSION FUNCT(500)
1  FORMAT(5X,12,8X,F6.3,2X,E12.5)
4  FORMAT(1H1, *INCLINATION INTERCEPT    AMPLITUDE*/ )
PRINT 4
5  CALL PLOT (.5,0.2,2)
DO 51, I=1,2
CALL PLOT (- 7.,-1.0,1)
CALL PLOT (- 5.,-1.,3)
CALL PLOT ( 5.,-1.,4)
CALL PLOT ( 5.,1.,4)
CALL PLOT (- 5.,1.,4)
CALL PLOT (- 5.,-1.,4)
CALL PLOT (- 5.,0.,3)
CALL PLOT ( 5.,0.,4)
CALL PLOT (0.,-1.,3)
CALL PLOT (0.,1.,4)
CALL PLOT ( 6.5,0.7,3)
DO 47, J=10,100,10
IO = J-10
RIO = 3.1416*IO/180.
A = COS (RIO)
B = SIN(RIO)
FMAX=FMIN=0
DO 40, M=1,361
Y = (M-181)/40.
R = SQRT(Y*Y + 1.0)  R3=R*R*R      R5=R3*R*R
IF(1.EQ.2)400,401
400 FUNCT(M) = (2.0*B - B*Y*Y - 3.0*A*Y)/R5      GO TO 32
401 FUNCT(M) = (2.0*A*Y*Y - A - 3.0*B*Y)/R5
32 IF (FUNCT(M).GT.FMAX) 33,34
33 FMAX = FUNCT(M)
GO TO 40
34 IF (FUNCT(M).LT.FMIN) 35,40
35 FMIN = FUNCT(M)
40 CONTINUE
CONST = (FMAX-FMIN)
ZEROPT = FUNCT(181)/CONST
PRINT 1, IO, ZEROPT, CONST
M=1
Y=-4.50
X= FUNCT(M)/CONST
CALL PLOT (Y,X,3)
45 Y=Y+0.025
M=M+1
X= FUNCT(M)/CONST
CALL PLOT(Y,X,4)
48 IF (Y.LT.4.5) 45,47
47 CONTINUE
51 CALL PLOT(-7.0,2.0,3)
98 END

```

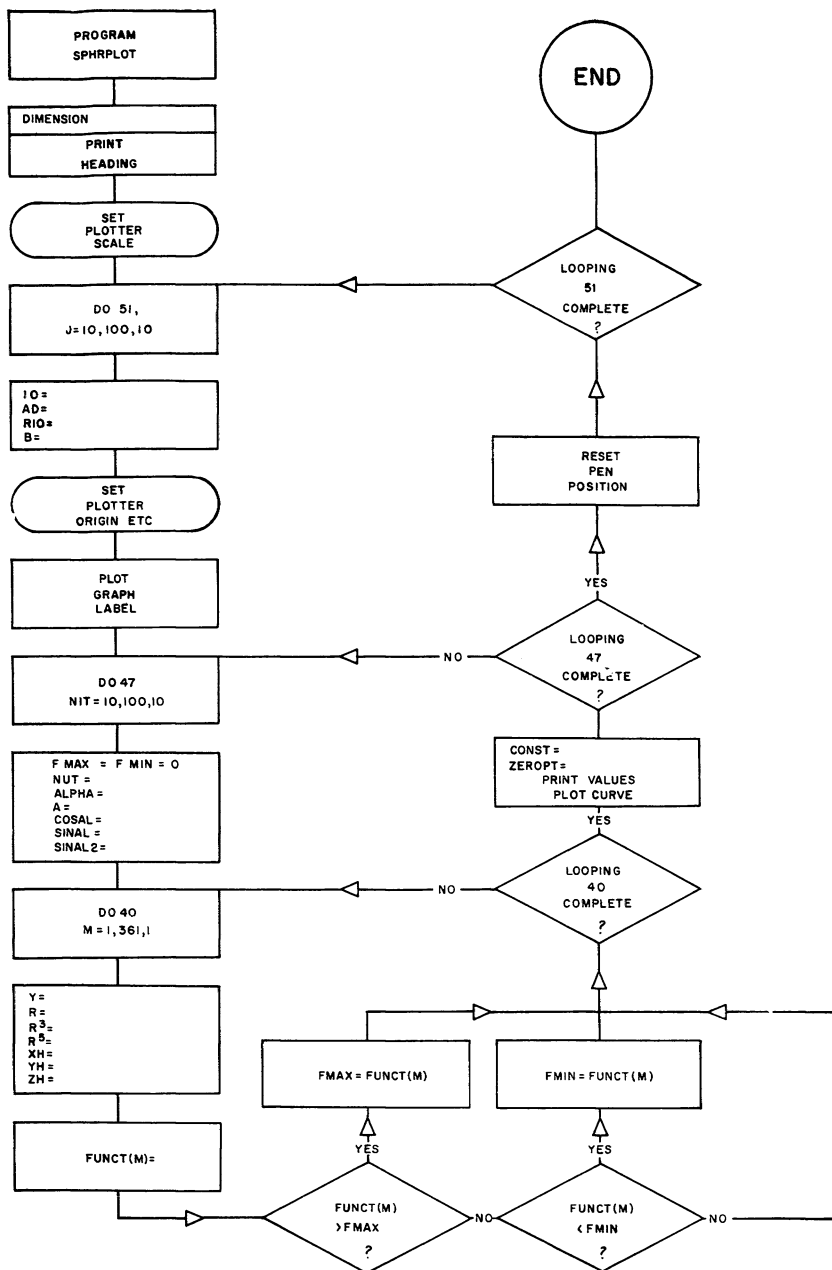


FLOW DIAGRAM-PROGRAM XZ PLOT


```

PROGRAM SPHRPLOT
DIMENSION FUNCT(500)
1  FORMAT(5X,12,10X,12, 5X,E12.5,4X,F6.3)
4  FORMAT(1H1, *INCLINATION   STRIKE      AMPLITUDE   INTERCEPT*/)
7  FORMAT(1HH,12)
PRINT 4
5  CALL PLOT (.5,0.2,2)
DO 51, J=10,100,10
  IO = J-10
  RIO = 3.1416*IO/180.
  AD= COS (RIO)
  B = SIN(RIO)
  CALL PLOT (- 7.,-1.0,1)
  CALL PLOT (- 5.,-1.,3)
  CALL PLOT ( 5.,-1.,4)
  CALL PLOT ( 5.,1.,4)
  CALL PLOT (- 5.,1.,4)
  CALL PLOT (- 5.,-1.,4)
  CALL PLOT (- 5.,0.,3)
  CALL PLOT ( 5.,0.,4)
  CALL PLOT (0.,-1.,3)
  CALL PLOT (0.,1.,4)
  CALL PLOT ( 6.5,0.7,3)
  ENCODE(3,7,CCC)IO
  CALL TEXT(CCC,3,3)
  DO 47,NIT=10,100,10
    NUT=NIT-10
    ALPHA = NUT *3.1416/180.0
    A=AD*COS(ALPHA)
    COSAL=COS(ALPHA)
    SINAL=SIN(ALPHA)
    SINAL2=SINAL*SINAL
    FMAX=FMIN=0
    DO 40, M=1,361
      Y = (M-181)/40.
      R = SQRT(Y*Y + 1.0)  R3=R*R*R      R5=R3*R*R
400  XH=(2.0*Y*Y-1.0)*A*COSAL/R5
      YH=-AD*SINAL2/R3
      ZH=-3.0*B*Y*COSAL/R5
      FUNCT(M)=XH+YH+ZH
32  IF (FUNCT(M).GT.FMAX) 33,34
33  FMAX = FUNCT(M)
      GO TO 40
34  IF (FUNCT(M).LT.FMIN) 35,40
35  FMIN = FUNCT(M)
40  CONTINUE
      CONST = (FMAX-FMIN)
      ZEROPT = FUNCT(181)/CONST
      PRINT 1,IO,NUT,CONST,ZEROPT
      M=1
      Y=-4.50
      X= FUNCT(M)/CONST
      CALL PLOT (Y,X,3)
45  Y=Y+0.025
      M=M+1
      X= FUNCT(M)/CONST
      CALL PLOT(Y,X,4)
48  IF (Y.LT.4.5) 45,47
47  CONTINUE
51  CALL PLOT(-7.0,2.0,3)
88  END

```



FLOW DIAGRAM - PROGRAM SPHRPLOT